

University of Maryland Mechanical Engineering

The Tunnel

Independent Research Project for ENME 488

Nate Crispell & Gerald Mace
Spring 2019

Introduction

The following report is intended to serve four main purposes. First, it will describe the motivation and learning outcomes of the tabletop wind tunnel project. Second, it will briefly describe the design and construction process of the wind tunnel in its current form. Third, it will detail the operation of the current design. Fourth, it will provide guidelines for recommended future changes and updates to the design.

Motivation

The goal of the project and the requirement for receiving credit for ENME 488 was to modify the rudimentary wind tunnel into one that functioned off of a closed feedback loop. The tunnel would be able to produce the users specified speed through the outlet of the tunnel regardless of ambient air conditions, thermal load of the hardware, or the geometry of the work piece being tested. A user would be able to control the testing conditions of their work piece no matter how the outlet was obstructed by the test subject. Additionally, knowing that this would require new hardware that the team could manipulate and code, the team decided to aim towards increasing the outlet max speed from 4 m/s to 10 m/s. Increasing the speed of the tunnel wasn't as important as creating a closed loop control system but was still an interesting goal for the team to work towards and benchmark with. These design goals were relevant throughout each phase of planning, research, and development of the wind tunnel.

Ultimately this project is most fundamentally to act as a learning opportunity. It has provided a valuable chance to apply concepts from technical classes in a physical space. The development of a mathematical model of the flow of air through the tunnel honed our understanding of fluid dynamics. The design of the motor control system did the same for mechatronics. The design and construction of the motor mount and platform gave hands on experience with machining and prototyping. Lastly, the reports and weekly meetings gave an opportunity for the team to further develop communication and technical writing skills. This project was a valuable experience which tied our engineering studies into a single tangible idea and we hope that this project is similarly engaging to other students as well.

Design

The design of the wind tunnel has been an iterative process informed by the results of data collection and by advice from Dr. Kiger, Dr. Larsson, and Majid Aroom. The first half of the semester involved creating a mathematical model of the tunnel in order to predict its performance and allow the team to appropriately size the equipment. The results of this modeling are provided in previous interim reports and were used to justify the selection of the hardware used in the design. The second half of the semester involved the selection and purchasing of the components and a final phase of concept generation before construction began. The design process was unfortunately slightly rushed due to the aggressive school schedules of the team. With that being said, the final physical layout of the wind tunnel is sound and was able to complete all required functions.

Hardware Selection

The Results of the Hardware selection process are presented below.

Motor – Turnigy Aerodrive SK3 – 5055 280KV Brushless Outrunner Motor

This motor has a maximum power output of 1510 Watts, far exceeding the power requirements of the project. The 280KV number refers to the no-load rpm per volt. Since this motor will be operating at a maximum of around 13 Volts, this means it has a maximum speed of ~3600 rpm. This is sufficient to generate the desired flow speed.



Figure 1: Image of motor

Electronic Speed Control and Connectors (\$21.07 + \$3.27)

The ESC connects the power supply to the motor and regulates it with the Arduino code using the Arduino's PWM output. The ESC can handle a maximum constant current of 60 amps. The gold connectors are a standard piece of equipment in the hobby motor space that allow large transfers of current and make assembly/disassembly of the component connections simple.

4mm Gold Connector



Figure 2: Gold Connectors



Figure 3: Speed Controller

Eyeboot 12 V 50 A 600 W – Power Supply

This is a switching power supply that will function as an AC to DC converter. According to the new mathematical model, 134 W is all that is required to produce more than 10 m/s. This would equate to a current draw of 11.2 A.



Watt meter and Power Analyzer (\$29.95)

Figure 4: Power supply



Figure 5: Watt meter

By wiring a watt meter in series between the power supply and speed control, the current can be monitored to ensure that the system is not attempting to draw past its limits.

20x10 Wood Propeller (\$8.83)

This propeller has a 20" diameter which means it would fit with a half inch tip clearance. The propeller has a 10" pitch. Propellers with 8" and 6" pitches are also available but will move 20-40% less air.

It was discovered later in this process that the inlet portion of the tunnel was 20 inches in diameter, not 21 inches as stated in the literature provided with the tunnel.



Figure 6: 10" pitch propeller

SDP1000-L05 – Differential pressure sensor



Figure 7: Image of the pressure sensor

This differential pressure sensor has a range of -5 Pa to 125 Pa.

Using $V_{outlet} = \sqrt{2P/(\rho(0.75 + .25k))}$, $\rho = \text{density of air}$, P is pressure measured by sensor, k is loss coefficient of screen downstream of first pressure tap. This equation was derived from Bernoulli's equation as applied to this tunnel with the pressure taps at the current location.

This pressure range corresponds to a velocity range of 0 m/s to 13 m/s which exceeds the initial design goals. The sensor has an error of 1.5% of the measured value at pressures greater than 10 Pa or 3.7 m/s or 0.2% of the full scale, whichever is greater. The resulting error in velocity measurements is presented in the graph below.

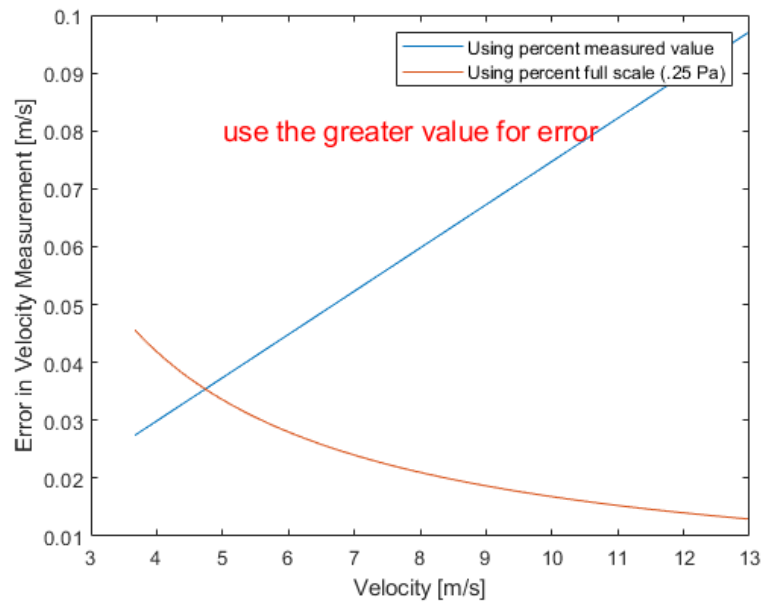


Figure 8: Error in velocity measurement resulting from the error in the pressure sensor reading.

As can be seen in the detail below, the error in velocity increases dramatically as the velocity decreases, even assuming the 0.25% F.S. is accurate at the lowest differentials.

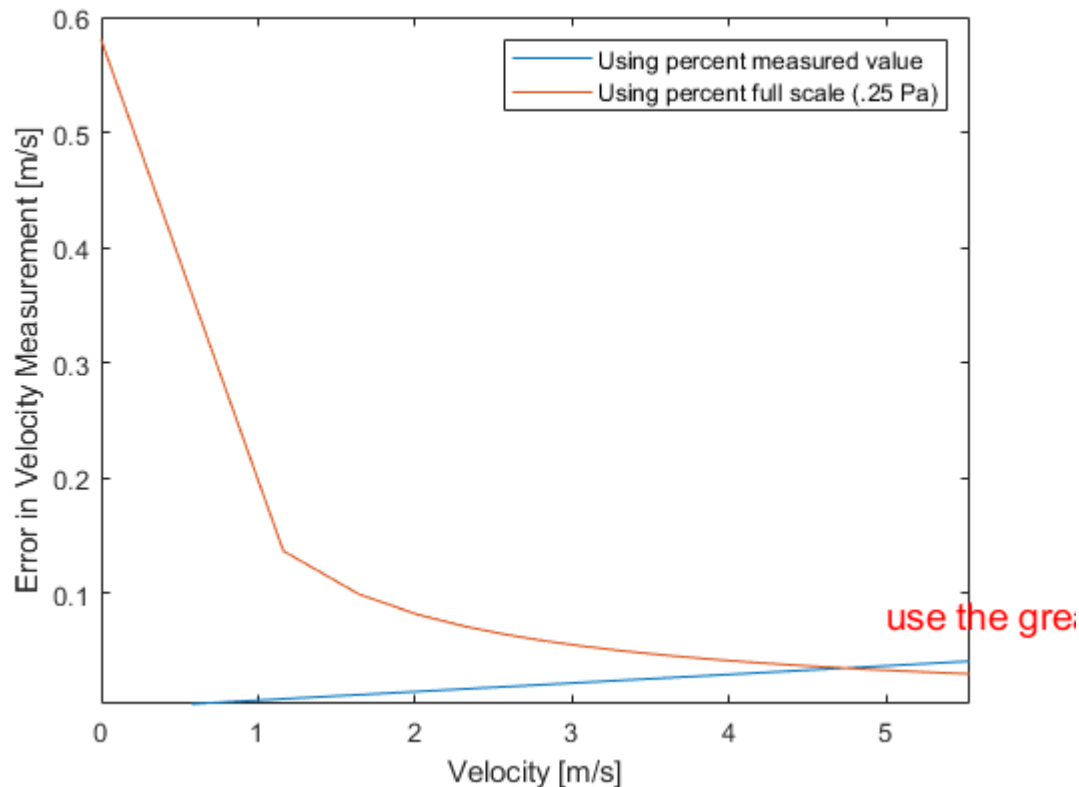


Figure 9: Low velocity error. The error increases significantly as the pressure differential drops below 10 Pa

Motor mount construction:

Because of the performance benefits of ducted propellers over non-ducted propellers, it was decided that the propeller should sit within the inlet portion of the tunnel. This should result in better performance, but it introduces a major risk. If the position of the propeller relative to the inlet of the tunnel is not locked and the propeller impacts the tunnel, it will likely destroy the inlet. This was not tested. While the first instinct of the team was to fix the motor mount to the tunnel itself this was non-ideal. The tunnel is 3-D printed, but it is not solid plastic. To reduce weight and cost, the tunnel is mostly hollow inside with a lattice connecting the solid walls of the pieces. Because of this, the tunnel is relatively weak and it is not possible to reliably fasten anything to the walls. It is also unwise to make any cuts in the walls of the tunnel, as this could reduce the stiffness of the whole section.

Fortunately, Majid (Chief) Aroom, the engineer who runs the undergraduate machine shop and was fundamental to the success of the project, had an idea. Rather than attempting to fix the motor mount to the tunnel itself, both the motor mount and the tunnel would be fixed to the same base. Not only does this solve the problem of relative position, it reduces the overall complexity for a user.

Setup

The current layout of the motor looking into the inlet is laid out below. The philosophy being employed is that a picture is worth 1000 words, so this is a few pages at least. The different components are described in the above sections.

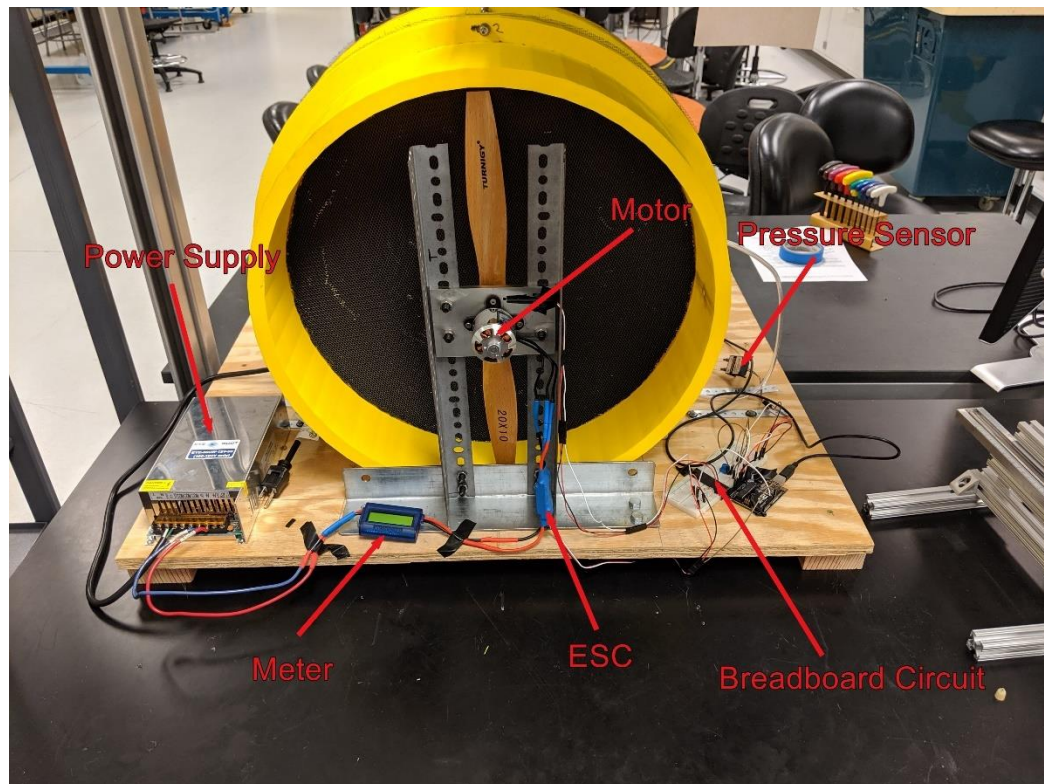


Figure 10: Hardware layout

Below is a detail of the tachometer setup. The Hall effect sensor must be pointed towards the magnet and must be close enough to the magnet to produce a reading. To ensure this is the case, reduce the `maxcount` variable (initialized before the `voidSetup` section in each variation of the code) to 5 and spin by hand 5 times to check that everything is working. This is not a particularly robust arrangement, so this may be a good area of focus for future development.

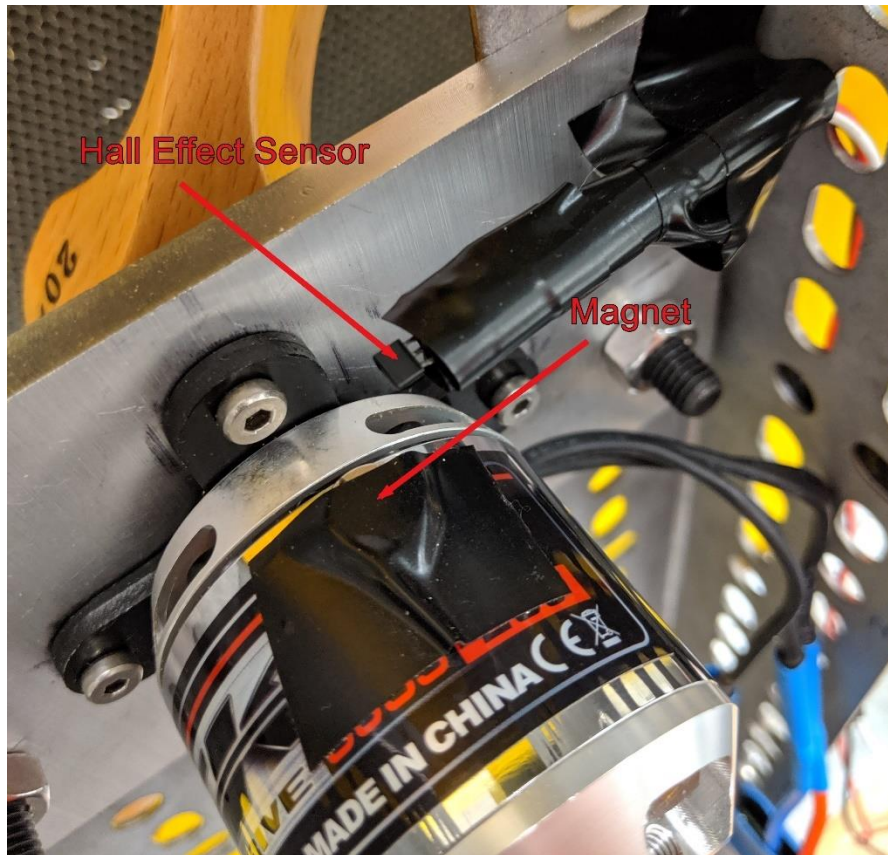


Figure 11: Tachometer setup. The rounded side of the sensor must be pointed directly towards the magnet.

Below is a detail of the power supply wiring. First, this does not need to be modified in any way to make the motor work. The two wires labeled **Ground** are on a common ground. The **Hot** and **Neutral** wires carry the charge. The **Ground** and **Power Out** wires connect to the Meter.

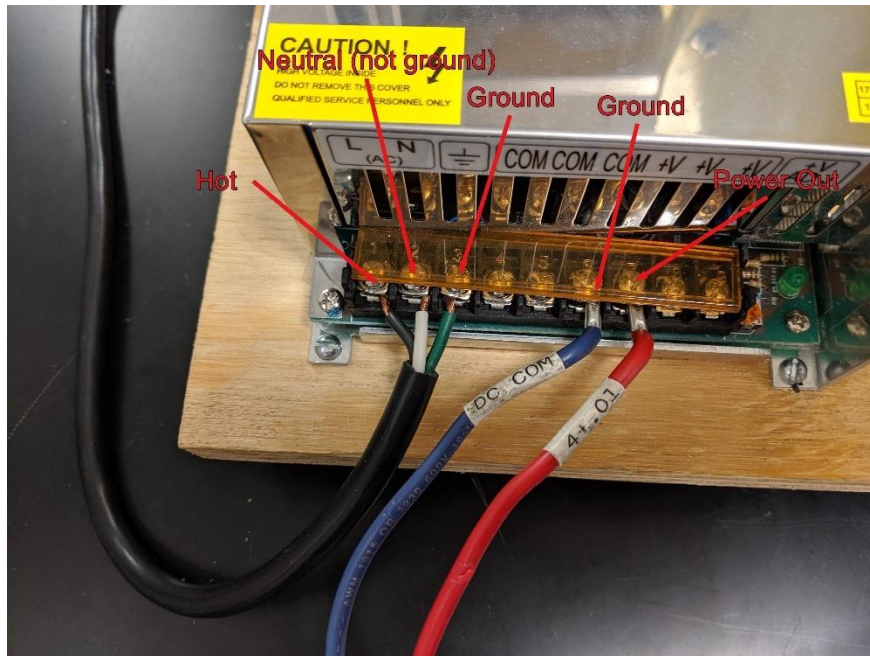


Figure 12: Wire layout for power supply

Below is a detail of the Meter. This has a readout for Voltage, Current, and Power. Disregard the Ah reading. The power and ground to ESC are the power and ground to ESC.

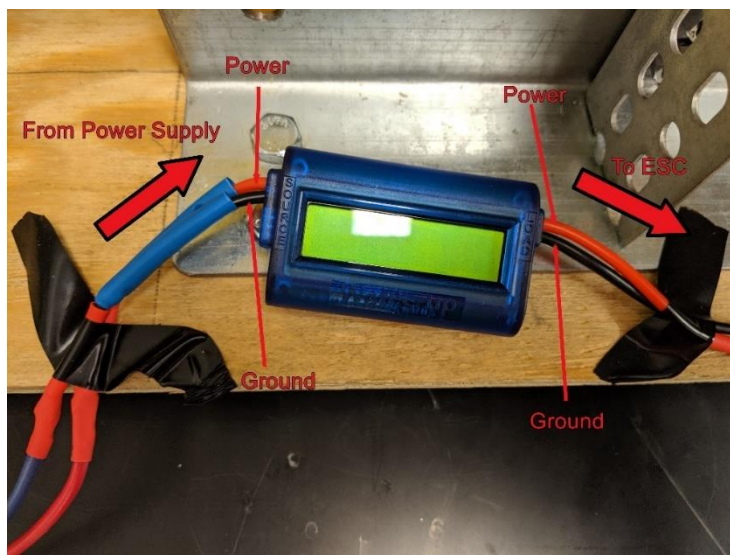


Figure 13: Wire layout for the watt meter

Below is the detail of the ESC. The three wires attached to the top can be in any order. Changing the order of the wires may change the direction of the motor rotation. However, there is no reason to touch this setup.

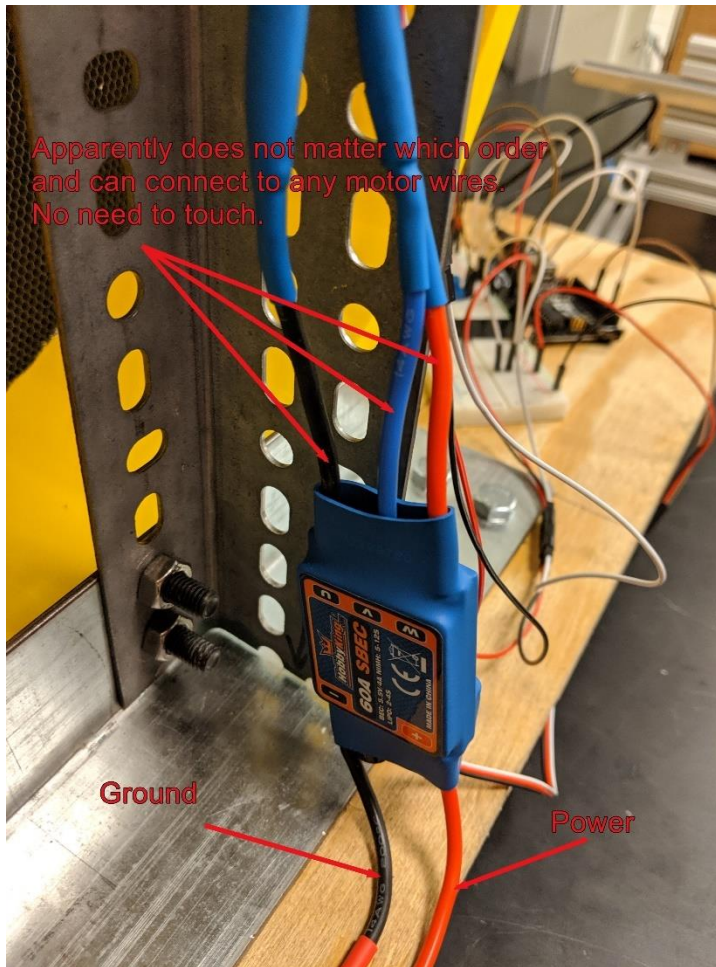


Figure 14: Explanation of wiring for the ESC

Operation

To start:

1. Ensure the Arduino does not have code that tells the motor to spin
 - a. If using a potentiometer to control the motor speed, set it to zero.
 - b. If you have previously loaded a code onto the Arduino that tells the motor to spin at a certain speed, it will start that code when it is powered on.
2. Check the bolt holding the propeller is properly tightened. We recommend marking the relative position of the bolt, washer, and propeller with a line across all three to help check for slipping.
3. Plug in the power supply. Make sure you hear the fan in the power supply running.
4. Upload the code.
5. Enjoy the high-pitched whine of the tunnel and feel the breeze.

Troubleshooting:

The motor controller is beeping:

It beeps on startup. However, different beep patterns mean different things. You can find beep codes online to help determine the exact issue. Usually the solution is to restart the whole system.

The Code

Function and description:

Through the process of testing and prototyping the wind tunnel, three different functioning codes were created. All three codes read and produced the rpm and pressure that the tunnel was currently experiencing, but they differed in how they would interact with the user and what the goal of that script was. The first code was to drive the motor at a speed relative to the position of a potentiometer. This code allowed the team to evaluate the velocity profile produced in the outlet at different motor rpms.

The second code increments the speed of the motor up by a designated amount and prints off the pressure and velocity calculated at that speed. This code was useful in seeing the performance of the tunnel and to graph the outlet velocity produced by the tunnel according to the inputted speed angle of the motor. This test gave the team a relationship between those two values which was used in the closed loop control of the system.

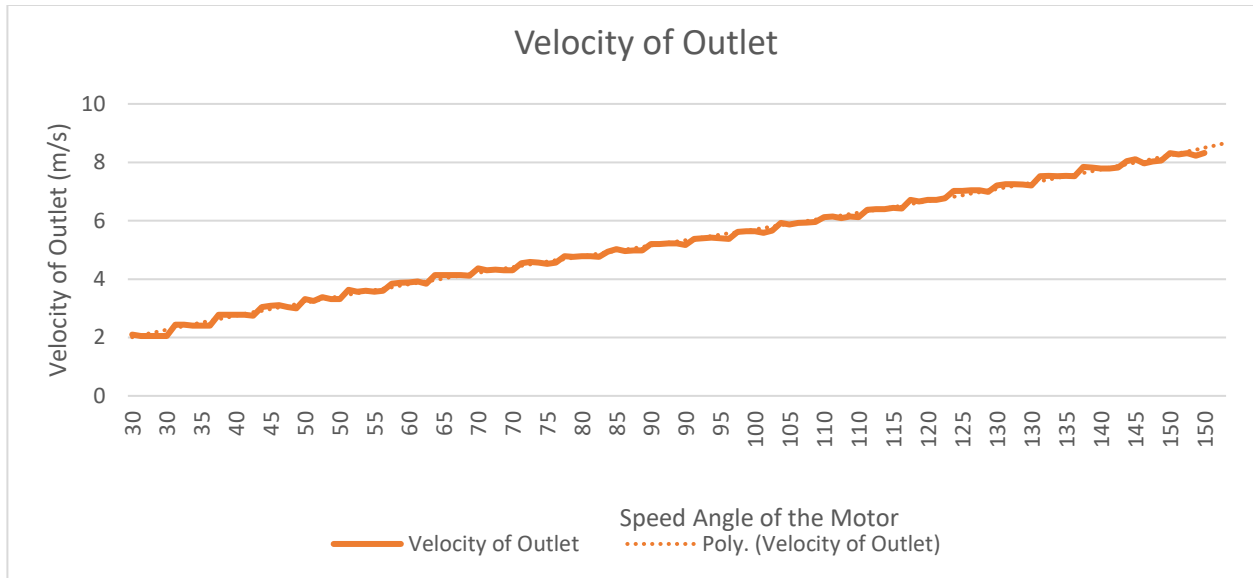


Figure 15: Data acquired relating outlet velocity with the speed angle given to the motor. This graph produced a line of best fit equation which was then used for the closed loop code.

The last code would allow the motor to rise up to speed in order to produce the airflow velocity designated by the user. The speed angle required by the motor is solved for with the relationship found in the previous code relating speed angle and output velocity. The code would then increment or decrement this speed angle in order to produce the actual velocity which was designated. The system is constantly sensing the pressure and solving for the output velocity according to the sensor at the outlet. If this value was higher or lower than what was designated by the user, the system would adjust.

The code was printed into pdf format and commented out in order to describe the function of each line, loop, and variable. To further advance the accuracy of the code, a PID controller could be implemented to fine tune the accuracy of the output. In addition, a high pass filter could be implemented to increase the accuracy of the pressure readings. In the current iteration of the closed loop, it is not known the exact accuracy of the velocity measurements being produced by tunnel but are assumed to be ± 0.5 m/s with the true output determined with an anemometer. What can be said is that the current tunnel will attempt to correct the output speed within a user designated amount. So far, the team tested this function within a relative output accuracy of 0.1 m/s.

Tunnel Iterations and Tests

Testing Method

One of the teams first projects was to create a testing apparatus that would mount a pitot tube and make fine movements so that the tunnels velocity profile could be tested and described through data collection. Once the pitot tube was mounted to the apparatus, a anemometer was then connected to the pitot tube with rubber tubing attached to its positive and negative terminals. The tip of the pitot tube was placed an inch away from the outlet of the tunnel with the thought that this would be the same distance that a test subject would be placed. The anemometer would then average the pressure readings over the span of ten seconds and a recording would be made. The pitot tube would then be incremented either up and down or left and right by 2 centimeters and the pressure would be averaged and recorded again. In later tests of the tunnel, this process was changed from being the entire profile of the outlet to just a “cross” formation due to the symmetry the profile was displaying.

Iteration 1:

The first model of the wind tunnel was composed of the 3-D printed shell placed on a lab table (*figure 16*), a box fan propped in place with 80-20 hardware (*figure 17*), and an 80-20 instrument holder to hold a pitot-static tube (*figure 18*). Velocity measurements were taken with a pitot-static tube attached to an Extech HD350 handheld anemometer. The only flow conditioning included in the tunnel was the 1.5 inch flow straightening hexagonal mesh press-fit into the second section of the tunnel (*figure 19*).



Figure 16: Figures 16-19 different views of the original tunnel setup



Figure 17. 20" box fan

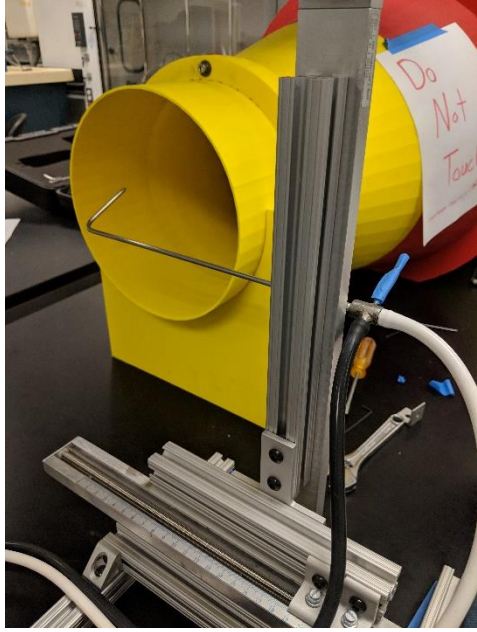


Figure 18. The aluminum 80/20 test rig with the mounted pitot tube.

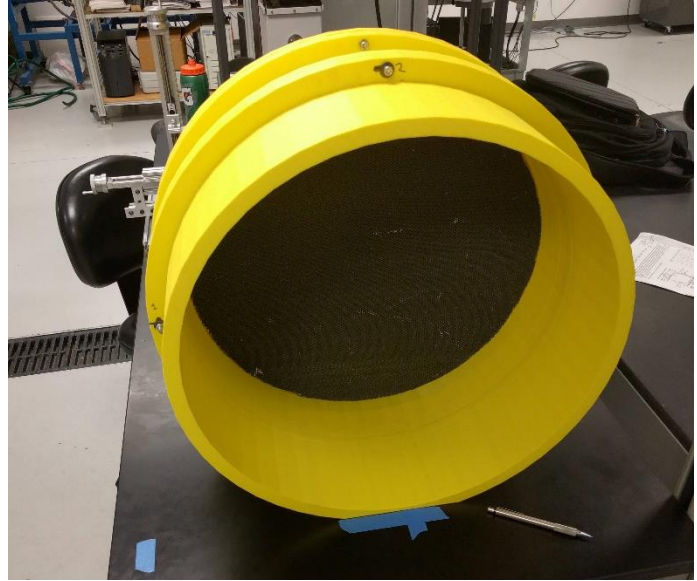


Figure 19. The press fit flow straightener.

The results of the first tests are shown in *table 1*. The data was collected data in a 12x12 square grid using Excel. Measurements were taken every 2 cm across the entire exit portion of the tunnel. The values presented are 10 second averages produced by the average function on the HD350. The maximum velocity produced was 3.5 m/s and the minimum velocity was 3.1 m/s. anomalous values at the very edges were disregarded because they were not fully within the flow at the exit. The percent variation was 12% with the highest values occurring at the outermost edges of the flow.

In this test, the flow was shown to be radially symmetric. This indicated that future measurements could be taken only along the center axes which would make testing simpler and shorter.

| | 0 | 2 | 4 | 6 | 8 | 10 | 12 | 14 | 16 | 18 | 20 | 22 | 24 |
|----|---|------|------|------|------|------|------|------|------|------|------|------|------|
| 0 | 0 | 0 | 0 | 0 | 0 | 0 | 2.3 | 0.44 | 0 | 0 | 0 | 0 | 0 |
| 2 | 0 | 0 | 0 | 2.98 | 3.4 | 3.4 | 3.41 | 3.42 | 3.43 | 3.39 | 0 | 0 | 0 |
| 4 | 0 | 0 | 3.29 | 3.38 | 3.37 | 3.35 | 3.33 | 3.33 | 3.39 | 3.43 | 3.45 | 0 | 0 |
| 6 | 0 | 0 | 3.41 | 3.36 | 3.35 | 3.3 | 3.26 | 3.26 | 3.28 | 3.37 | 3.43 | 3.47 | 0 |
| 8 | 0 | 3.47 | 3.42 | 3.32 | 3.25 | 3.22 | 3.18 | 3.17 | 3.19 | 3.3 | 3.4 | 3.45 | 0 |
| 10 | 0 | 3.5 | 3.38 | 3.25 | 3.19 | 3.18 | 3.11 | 3.12 | 3.15 | 3.25 | 3.37 | 3.39 | 0 |
| 12 | 0 | 3.48 | 3.38 | 3.23 | 3.17 | 3.13 | 3.09 | 3.1 | 3.14 | 3.22 | 3.35 | 3.41 | 2.51 |
| 14 | 0 | 3.5 | 3.44 | 3.29 | 3.2 | 3.13 | 3.18 | 3.12 | 3.13 | 3.16 | 3.29 | 3.34 | 2.51 |
| 16 | 0 | 3.48 | 3.44 | 3.34 | 3.25 | 3.19 | 3.19 | 3.22 | 3.22 | 3.26 | 3.36 | 3.42 | 0 |
| 18 | 0 | 0 | 3.43 | 3.4 | 3.29 | 3.26 | 3.26 | 3.27 | 3.29 | 3.35 | 3.38 | 3.32 | 0 |
| 20 | 0 | 0 | 3.31 | 3.44 | 3.38 | 3.36 | 3.35 | 3.35 | 3.36 | 3.38 | 3.42 | 0 | 0 |
| 22 | 0 | 0 | 0 | 0.8 | 3.41 | 3.37 | 3.39 | 3.39 | 3.43 | 3.08 | 0 | 0 | 0 |
| 24 | 0 | 0 | 0 | 0 | 0 | 0 | 0 | 0 | 0 | 0 | 0 | 0 | 0 |

Table 1. Results of first test. As shown by the value generated heatmap,

Iteration 2:

The only modification to the tunnel between this test and the previous was the sanding of the junction between the contraction section and the outlet. The data showed no significant change in flow.

Iteration 3:

The third iteration of the tunnel included the addition of window screen at the junction of the inlet piece and the second section, and the second section and the contraction (*figure 20*). The flow straightener was placed upstream of the screens in the inlet section (*figure 21*).

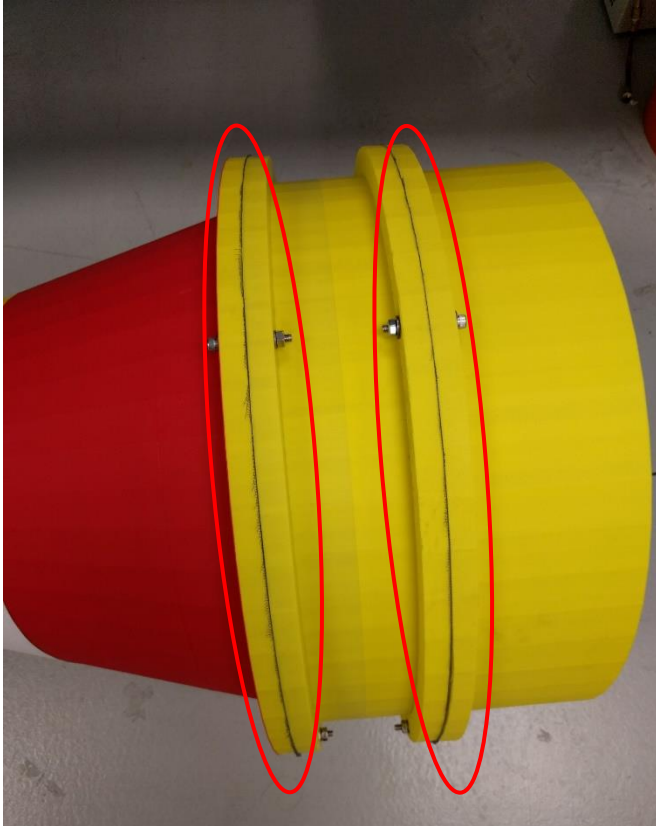


Figure 20: Area where screens were placed



Figure 21: View of flow straightener

| y (cm) | x (cm) | | | | | | | | | | | | |
|-----------|--------|------|------|------|------|------|------|------|------|------|------|------|------|
| | 0 | 2 | 4 | 6 | 8 | 10 | 12 | 14 | 16 | 18 | 20 | 22 | 24 |
| 0 | | | | | | | 3.12 | | | | | | |
| 2 | | | | | | | 4.05 | | | | | | |
| 4 | | | | | | | 4.07 | | | | | | |
| 6 | | | | | | | 4.05 | | | | | | |
| 8 | | | | | | | 4 | | | | | | |
| 10 | | | | | | | 4.01 | | | | | | |
| 12 | 2.54 | 4.02 | 4.03 | 4.04 | 4.03 | 4.01 | 4 | 4.02 | 4.02 | 4.03 | 4.03 | 4.04 | 3.09 |
| 14 | | | | | | | 3.99 | | | | | | |
| 16 | | | | | | | 4.01 | | | | | | |
| 18 | | | | | | | 4.04 | | | | | | |
| 20 | | | | | | | 4.03 | | | | | | |
| 22 | | | | | | | 4.03 | | | | | | |
| 24 | | | | | | | 3.23 | | | | | | |

Table 2. Result of third round testing

The data collected showed a significant improvement in the uniformity of the velocity profile as shown in *table 2*. The maximum velocity was 4.07 m/s and the minimum velocity was 3.99 m/s, excluding anomalies at the edges. This is a percent variation of only 1.97% across the outlet, a significant improvement from previous results. However, this test also showed significant time variation of the velocity. It was noted but not recorded that the velocity increased by roughly 1 m/s over the span of about 45 minutes. This led to the decision to design the motor control system to help maintain a constant velocity before attempting other design changes to modify the flow.

After the closed loop motor control system was designed and implemented, measurements were taken to characterize the new flow field. *Tables 4.a, 4.b, and 4.c* show the resultant velocity profiles at 1500 rpm, 2080 rpm, and 2790 rpm respectively. The minimum and maximum speeds are tabulated in *table 3* below. The percent variation across the velocity profile did increase at all three tested speeds, most likely as a result of the dramatically different blade used to drive the air. This increase in variation could be solved by exploring the different blades or by modifying the passive flow controls in the tunnel. The data below disregards some outlying data collected at the very edge of the tunnel. The readings were most likely the result of the boundary layer between the outlet flow and the still air surrounding it, rather than air directly driven by the blade.

| | 1800 rpm | 2080 rpm | 2790 rpm |
|------------------------|----------|----------|----------|
| Maximum Velocity (m/s) | 4.46 | 6.49 | 8.84 |
| Minimum velocity (m/s) | 4.29 | 6.21 | 8.47 |
| % var | 3.81 | 4.31 | 4.19 |

Table 3. Maximum and minimum velocity measurements and 1800, 2080, and 2790 rpm.

This test also showed an asymmetry in the velocity data across the vertical axis with higher velocity readings on the left side of the outlet tunnel than on the right. It may be beneficial for future students to take another test of the entire profile to gain insight on the source of this anomaly.

a)

| | x (cm) | | | | | | | | | | | | |
|--------|--------|------|------|------|------|------|------|------|------|------|------|------|-----|
| y (cm) | 0 | 2 | 4 | 6 | 8 | 10 | 12 | 14 | 16 | 18 | 20 | 22 | 24 |
| 0 | | | | | | | | | | | | | |
| 2 | | | | | | | 4.46 | | | | | | |
| 4 | | | | | | | 4.44 | | | | | | |
| 6 | | | | | | | 4.4 | | | | | | |
| 8 | | | | | | | 4.38 | | | | | | |
| 10 | | | | | | | 4.35 | | | | | | |
| 12 | | 4.38 | 4.42 | 4.41 | 4.39 | 4.33 | 4.34 | 4.29 | 4.33 | 4.37 | 4.37 | 4.41 | 4.3 |
| 14 | | | | | | | 4.35 | | | | | | |
| 16 | | | | | | | 4.36 | | | | | | |
| 18 | | | | | | | 4.39 | | | | | | |
| 20 | | | | | | | 4.43 | | | | | | |
| 22 | | | | | | | 4.42 | | | | | | |
| 24 | | | | | | | 3.37 | | | | | | |

b)

| | x (cm) | | | | | | | | | | | | |
|--------|--------|------|------|------|------|------|------|------|------|------|------|-----|----|
| y (cm) | 0 | 2 | 4 | 6 | 8 | 10 | 12 | 14 | 16 | 18 | 20 | 22 | 24 |
| 0 | | | | | | | 2.99 | | | | | | |
| 2 | | | | | | | 6.31 | | | | | | |
| 4 | | | | | | | 6.3 | | | | | | |
| 6 | | | | | | | 6.28 | | | | | | |
| 8 | | | | | | | 6.25 | | | | | | |
| 10 | | | | | | | 6.22 | | | | | | |
| 12 | 5.93 | 6.41 | 6.49 | 6.49 | 6.37 | 6.24 | 6.21 | 6.23 | 6.32 | 6.37 | 6.32 | 6.3 | 0 |
| 14 | | | | | | | 6.24 | | | | | | |
| 16 | | | | | | | 6.27 | | | | | | |
| 18 | | | | | | | 6.37 | | | | | | |
| 20 | | | | | | | 6.43 | | | | | | |
| 22 | | | | | | | 6.39 | | | | | | |
| 24 | | | | | | | 5.36 | | | | | | |

c)

| | x (cm) | | | | | | | | | | | | |
|--------|--------|------|-----|------|-----|------|------|-----|------|------|------|-----|----|
| y (cm) | 0 | 2 | 4 | 6 | 8 | 10 | 12 | 14 | 16 | 18 | 20 | 22 | 24 |
| 0 | | | | | | | 4.82 | | | | | | |
| 2 | | | | | | | 8.66 | | | | | | |
| 4 | | | | | | | 8.61 | | | | | | |
| 6 | | | | | | | 8.6 | | | | | | |
| 8 | | | | | | | 8.56 | | | | | | |
| 10 | | | | | | | 8.49 | | | | | | |
| 12 | 7.78 | 8.79 | 8.8 | 8.84 | 8.7 | 8.52 | 8.47 | 8.5 | 8.67 | 8.76 | 8.66 | 8.6 | 0 |
| 14 | | | | | | | 8.5 | | | | | | |
| 16 | | | | | | | 8.56 | | | | | | |
| 18 | | | | | | | 8.65 | | | | | | |
| 20 | | | | | | | 8.74 | | | | | | |
| 22 | | | | | | | 8.71 | | | | | | |
| 24 | | | | | | | 7.65 | | | | | | |

Table 4. a) Velocity readings at 1800 rpm. b) velocity readings at 2080 rpm. c) velocity readings at 2790 rpm

Mathematical model of the tunnel

The first step to designing a fan system for the tunnel was to create a mathematical model of the flow through the tunnel to derive power requirements to use for motor sizing. The full process for this and the Matlab code used to generate the following results are included in report 1.5. However, the results of the model are included below.

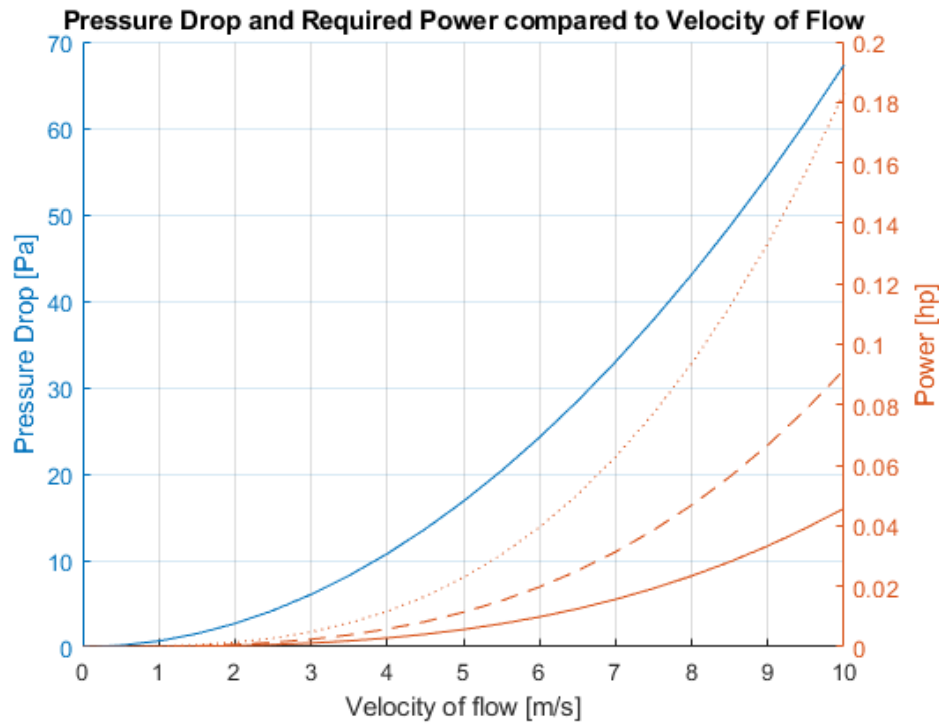


Figure 23: Pressure drop related to velocity. The solid, dashed, and dotted orange lines represent the power requirements at a fan efficiency of 25%, 50%, and 100%.

The results only require a motor power of around 0.18 hp or 134 Watts to generate an exit velocity of 10 m/s at 25% fan efficiency.

Conclusion

Closed Loop Function

The code to get the tunnel to function involves using data from a prior test on the velocity produced by the system at every possible speed angle the motor is programmed to function with. The user inputs a desired speed before running the closed loop control code. Using the line of best fit equation corresponding with the velocity vs. speed angle data, the code solves for the speed that the motor should be set to in order to produce the users desired velocity. Without torqueing the bolt, the tunnel increments itself up to that desired speed by increasing the speed angle five times a second. Once that speed is reached, the tunnel exits the setup loop and enters the control loop.

A pressure transducer produces a voltage drop which is read by the Arduino ADC as a 10-bit code. Using the full-scale range of the transducer and its known operating voltages, the code is turned into a value for the pressure the tunnel is currently producing at the outlet. The loop determines the velocity caused by this pressure drop by solving a variation of the Bernouli equation which is a function of the current pressure drop, the current air density in the environment (Specified by the user,) the geometry of the wind tunnels inlet and outlet sections, and the friction loss coefficient of the wind tunnels air straightening screens. The code runs through this calculation every time the tunnel runs through the specified number of rotations to determine rpm (this was set to 50 for every test done by the team but can be increased or decreased at will.)

The control loop subtracts calculated velocity from what the user specified in the setup loop. The idea was that the code would determine whether this difference was in the positive or negative direction and then would increment the speed accordingly. The current iteration of the code gets close to this but will require additional loops for perfect function. Initial tests done by the team displayed the tunnel incrementing and decrementing its speed when obstructions were placed or removed from the outlet section which was the initial goal of the project. Some more work will have to be done however.

Areas of Improvement

As mentioned, the design and construction phases of the tunnel's construction were during the second half of the semester. Some generated design concepts didn't come to complete fruition and some areas of the tunnels design could be improved upon further. In the interest of time and the team's goal of having a working final product, it was decided that these possible improvements would be laid out here in this final report for future students to start their journey if they decide to work on the tunnel in their research studies as well.

- Permanently attaching components to the base board: The electrical components such as the Arduino, breadboard, and pressure sensor are all loosely laying on the base board of the tunnel. This was only meant to be temporary for testing purposes and no

permanent attachments were made just in case design changes were made. After it was certain that no modifications would be made to this section of the tunnels function, then making these attachments permanent would help make the construction more robust.

- Improving the code to reduce steady state error and filter the information to improve accuracy of the control loop: The control loop variation of the tunnel code's function is explained earlier in this report. It doesn't function ideally, and will require more loops in order to have the speed increment and decrement correctly. Future team members can expand upon either the code or the physical layout of the components to include a PID controller and high pass filter to ensure the accuracy of the closed control loop as well.
- Print a new outlet to the tunnel which extends its length to be equal to one diameter: It was discussed in the early stages of the project to extend the outlet to ensure that the flow would be fully developed by the time it left the tunnel and made contact with the test subject. This was placed on the back burner so that the team could pursue the construction of the mechatronics side of the project. Final tests after the control loop was finalized showed that the new fan system was causing an uneven flow at the edges of the outlet that wasn't previously seen in previous iterations. New team members could look into the many possible problems/solutions that may exist to fix this problem, but the one that can be brought back to the front of the project timeline could be the extension of the outlet.
- Finding the problem with the tunnels velocity profile uniformity and solving it: With the new closed control loop system comes the problem that the velocity profile is no longer uniform. While it wasn't determined yet by the team, some guesses on what the cause of the problem is were theorized. It could be caused by any imbalance or asymmetry in the motor mount system. Any obstructions or uneven surfaces within the tunnel at the locations of the pressure taps could have possibly caused this as well. Possibly the placement of the hard ware could be causing some back pressure in the affected area as well. Future researchers could hypothesize and test the cause of the loss of uniformity and implement a solution to increase the tunnels accuracy and quality.

Final Thoughts

As mentioned in the introduction of this report, this project was a great way to combine subjects and concepts from our past engineering studies in an interesting way. The team was more than happy to be a part of this project and appreciated the opportunity to test our knowledge and to show our creativity in the design of the tunnel. While the areas of improvement may not be comprehensive of the necessary changes to make the tunnel the best it can be it is hopefully a good place to start for future researchers.

While the research is done in terms of the requirements for credit toward ENME 488, we insist on staying involved with the project to answer any questions and clarify any information about hardware, testing methods, or any possibly inquiry future team members would have about the tunnel. We believe the tunnel could be a useful resource for small labs on campus that need

to do velocity or turbulence testing on their small aircraft or aerodynamic components. The tunnel could also serve pedagogical purposes as well displaying concepts related to fluid dynamics or even mechatronics and controls. We hope that the tunnel can one day achieve high standards of reliability and sophistication in order to be used in these scenarios. We wish that this foundation is a reliable place to start for future researchers who work to improve not only the tunnel's performance but their own personal understanding of engineering concepts and practices.